JOURNAL OF APPLIED ELECTROCHEMISTRY **26** (1996) 369–377

Zinc removal from dilute solutions using a rotating cylinder electrode reactor

J. ST-PIERRE*, N. MASSÉ, É. FRÉCHETTE, M. BERGERON

INRS-Géoressources, 2700 Rue Einstein, Case Postale 7500, Ste-Foy, Québec, Canada, G1V 4C7

Received 3 January 1995; revised 15 August 1995

Mine residue recycling processes produce dilute zinc solutions suitable for metal recovery. The rotating cylinder electrode reactor behaviour sequentially followed charge transfer and diffusion control mechanisms, even with solutions contaminated with metals or organic substances. Zinc removal at low pH (~0) and low concentration (~2 mg dm^{-3}) is demonstrated. Under galvanostatic operation, the zinc deposition current efficiency in the charge transfer control region attains values up to 77.3%, whereas in the diffusion control region it decreases rapidly to values as low as 0.1%. When a potentiostatic mode is used, less energy is required to deposit zinc, even at low current efficiency. The results and possible problems for continuous reactor operation under conditions of powder formation are identified and discussed using knowledge from other zinc industries such as electrowinning, plating and batteries.

List of symbols

A_c cylinder electrode active surface (cm^2)
A_d disc electrode active surface (cm^2)
c_H analytical sulfuric acid concentration ($mol\,cm^{-3}$)
c_{Zn} analytical zinc sulphate concentration ($mol\,cm^{-3}$)
d cylinder electrode diameter (cm)
D zinc diffusion coefficient ($cm^2\,s^{-1}$)
F Faraday constant (96 500 $C\,mol^{-1}$)
I total current (A)
I_H hydrogen production current (A)
I_l zinc deposition limiting current (A)
j critical hydrogen current density ($A\,cm^{-2}$)
k zinc mass transfer coefficient ($cm\,s^{-1}$)
K Wark's rule constant
n number of electrons exchanged in the zinc deposition reaction
Re Reynolds number ($\omega d^2/2\nu$)
Sc Schmidt number (ν/D)
Sh Sherwood number (kd/D)
t time (s)
V electrolyte volume in the RCER (cm^3)
ν solution kinematic viscosity ($cm^2\,s^{-1}$)
ϕ zinc deposition current efficiency
ω rotation speed ($rad\,s^{-1}$)

1. Introduction

The rotating cylinder electrode reactor (RCER) has found applications in metal removal from dilute solutions due to a combination of features which are not shared by other reactors [1–4]. These include an easily operable compact design and ability to work under continuous conditions, producing a fluidized metal powder which is subsequently separated from the electrolyte. Selective extraction is also possible owing to a relatively uniform current distribution. Finally, the RCER is ideally suited for environmental clean-up since it operates in a concentration range which, at the lower end, corresponds roughly to legislation constraints (1 p.p.m.) and at the higher end (several 1000 p.p.m.) is larger than the concentration found in many industrial effluents.

Although the possibility of removing zinc has been mentioned in the literature [5, 6] and some processes were the object of patents [7–9], the operational data available (Table 1) are insufficient to tailor the technology to a particular problem since neither parameter selection nor reactor behaviour have been discussed. Others have reported data for zinc deposition from alkaline solutions [10–12], but these processes involve high metal concentrations typical of electrowinning practice, very low rotation speeds, or partially immersed cylinders. Therefore, the latter studies do not offer any RCER operational data of interest for the treatment of effluents.

The theoretical foundations of zinc deposition at low concentrations using an RCER are reported in this paper. To understand this process, the usefulness of the existing literature on zinc electrowinning, zinc based batteries and zinc plating involving highly concentrated solutions, is also demonstrated. This discussion is illustrated with recently obtained data for the treatment of sulphide-containing mine residues [13–15]. The hydrometallurgical treatment of the tailing pounds resulted in a solution enriched with dissolved metals. For the residues of Manitou (Val D'Or, Québec), zinc was identified for potentially economical retrieval [13–15]. Copper retrieval however, was

* Present address: Ballard Power Systems, 107-980 West 1st Street, North Vancouver, British Columbia, Canada, V7P 3N4.

0021-891X

Table 1. Operational data reported for zinc removal using a RCER [5, 7–9]

Reactor type	Undivided or divided, batch or continuous
Type of control	Galvanostatic* (50–5000 A m^{-2}) or potentiostatic (−1.7–−1.86 V vs Hg/Hg_2SO_4)
Rotation speed	62.8–1150 rad s^{-1} (600–11 000 r.p.m.)
pH	1–6.4
Temperature	298–333 K
Zinc concentration	61–8500† mg dm^{-3}
Current efficiency	5.5–100%
Zinc powder composition	55–73.6% Zn

* Based on the geometric surface area.
† Based on a solution density of 1 g cm^{-3}.

identified as an essential preliminary step before zinc recuperation. Problems related to copper recovery from a solution containing dissolved oxygen and several metallic ions using a RCER were discussed in previous publications [16–18]. The various alternative processes considered led to several solution chemistries. The experimental solutions were generated from a sulphide tailing, although for the purposes of comparison and discussion, synthetic solutions were also studied.

2. Experimental details

Most experiments were conducted at room temperature (295 ± 0.5 K) and normal atmospheric pressure unless otherwise noted.

2.1. *Solutions*

The solutions used were obtained from the washing step made prior to the flotation of the Manitou mining residues located at Val D'Or, Québec, Canada. The subsequent procedure pertaining to iron precipitation is described elsewhere [16]. The resulting solution was dilute sulphuric acid (pH 4) containing several metals where zinc was predominant (Table 2). This solution was then treated with different alternative processes as shown in Fig. 1. Copper present in relatively substantial quantities (Table 2) needs to be removed, otherwise it interferes with the subsequent steps of the process. Copper strongly binds with the extractant selected, and is therefore difficult to eliminate, leading to a loss in separation efficiency over time. Copper

*Table 2. Typical analysis of the washing solution after iron precipitation**

Element	*Concentration /mg dm^{-3}*
Zn	3800
Cu	55
Cd	16
Co	8.7
As	3
Fe	2.3

* Solution *a*, Fig. 1.

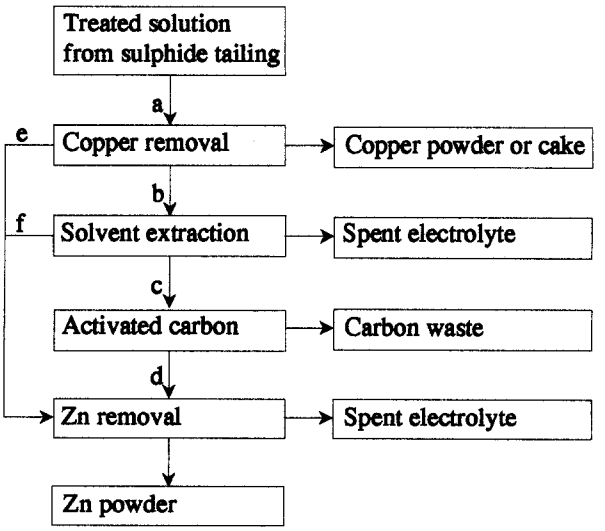

Fig. 1. Partial process diagram used to treat mine residues. Letters *a* to *f* refer to the different solutions discussed in the text.

also codeposits with zinc, resulting in a powder of lesser purity to the detriment of its selling price. Although several methods were used to remove copper (either by chromatography, cementation or by using a RCER) [15, 16] to obtain sufficiently pure zinc solutions suitable for electrolysis, the different process variants thus generated were not systematically studied. When considering solvent extraction, either cementation or the RCER are used (path *ae*, Fig. 1). In the other case, copper is removed by chromatography and the process is given by path *abf* (Fig. 1), although there may be a need for using an activated carbon cleaning step (path *abcd*, Fig. 1). The zinc current efficiency decreases significantly in the presence of minute amounts of dissolved organics. The composition of the solutions resulting from the different processes considered here is given in Table 3.

Synthetic solutions were prepared using reagent grade chemicals (H_2SO_4 and $ZnSO_4.7H_2O$) and deionized water (Millipore model Milli-Q Plus). The composition of these solutions is given in Table 3.

Solution analysis was performed by atomic absorption with an error of ± 10% and detection limits lower than 1 mg dm^{-3} for all the elements.

2.2. *Kinematic viscosity*

The kinematic viscosity was measured for some synthetic solutions (Table 3) with a calibrated Cannon–Fenske routine viscometer (no. 25) with a precision of ± 0.000 02 cm^2 s^{-1}. A thermostatic bath (Neslab model RTE-100) ensured constant temperature during measurements. The viscometer was immersed for at least 10 min before each measurement.

2.3. *Diffusion coefficient*

A zinc disc with a 0.196 cm^2 surface area imbedded in a PTFE cylinder was used to evaluate the zinc diffusion coefficient. A synthetic solution was used for these measurements (Table 3). The electrode was coupled to a rotating disc electrode system (Pine

Table 3. Zinc solutions composition, properties and electrochemical characteristics

*Solution**	*Zn conc* /mg dm^{-3}	*H_2SO_4 conc* /mol dm^{-3}	*Kinematic* viscosity /cm^2 s^{-1}	*Zn deposition* current efficiency† /%	*Zn mass transfer* coefficient /cm s^{-1}	*Zn diffusion* coefficient‡ /cm^2 s^{-1}
Synthetic	3800	? (pH 4)	0.00986	–	–	–
	5000	1	0.0114	39.9–50.7	$1.80–2.00 \times 10^{-3}$	$7.62–8.97 \times 10^{-7}$
f	6800	1	–	21.0	7.24×10^{-4}	1.85×10^{-7}
d	6800	1	–	46.3	1.04×10^{-3}	3.25×10^{-7}
e (copper removed with a RCER)	3800	? (pH 4)	–	42.7	–	–
e (copper removed by cementation)	5100	? (pH 4)	–	77.3	4.56×10^{-3}	2.99×10^{-6}

* See Fig. 1.
† In the charge transfer control region.
‡ Derived using the zinc mass transfer coefficient and Equation 14.

Instruments model AFMSRX). Platinum foils served as insoluble anodes so as to avoid solution contamination. The presence of anodically produced oxygen in the catholyte was reduced by separating the anodic and cathodic compartments with fritted glass. In addition, the catholyte was degassed with nitrogen both before and during experiments. A saturated calomel electrode (SCE) was used as a reference. Experiments were carried out with a Schlumberger 1286 electrochemical interface controlled via a PC microcomputer using Corrware software. The rotation speed was varied from 83.8 to 670 rad s^{-1} (800 to 6400 r.p.m.) to determine the limiting current variation for zinc deposition in the diffusion controlled region (−1.36 V vs SCE). The resulting currents obtained after two minutes are plotted against the square root of the rotation speed in Fig. 2. The Levich equation, modified to take into account a parallel charge transfer controlled reaction (hydrogen evolution) [19]:

$$I = I_H + 0.62nFA_d D^{\frac{2}{3}} \nu^{-\frac{1}{6}} c_{Zn} \omega^{\frac{1}{2}} \quad (1)$$

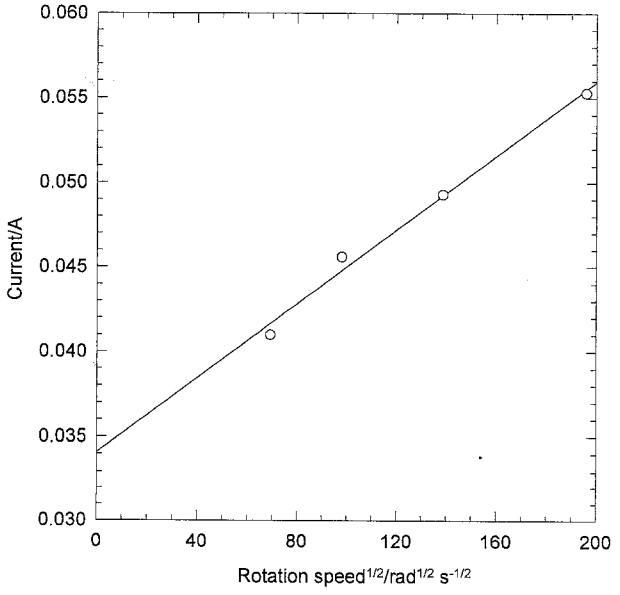

Fig. 2. Total current as a function of the square root of the rotation speed. 5 g dm^{-3} Zn as $ZnSO_4.7H_2O$ + 1 mol dm^{-3} H_2SO_4 at 295 K and −1.36 V vs SCE.

led to a zinc diffusion coefficient of 1.56×10^{-7} cm^2 s^{-1}.

2.4. *Cementation*

The cementation reactor was agitated (Caframo model RZR 50) and temperature controlled from 308 to 348 K (Section 2.2). Different quantities of zinc powder (99.5%) were added to the solutions (1 dm^3 of solution *a*, Fig. 1) using three different strategies. From $2\frac{1}{2}$ to thirty-two times the required stoichiometric amounts for the removal of all impurities (Table 2) were used. These quantities were then divided into equal parts to make either one, two or four additions, spaced 15 min apart and starting at the beginning of the experiments.

The cobalt concentration was monitored by taking small samples (10 cm^3) from the reactor; these were filtered and analysed by atomic absorption (Section 2.1). The total volume of the samples removed from the reactor was not large enough to seriously alter the initial quantity of electrolyte.

2.5. *Rotating cylinder electrode reactor*

The rotating cylinder electrode batch reactor consisted of an aluminium cylinder installed on a rotor. The cylinder was initially zinc plated from a 75 g dm^{-3} Zn as $ZnSO_4.7H_2O$ + 1 mol dm^{-3} H_2SO_4 solution (1 A, 30 min) and subsequently polished with a 600 grit paper. The aluminium electrode was mounted between two PTFE discs (each 1.27 cm long by 5.08 cm diam.) to eliminate edge effects. The exposed aluminium surface was 20.3 cm^2 (1.27 cm long by 5.08 cm diam.). A rotation speed of 168 rad s^{-1} (1600 r.p.m.) was used.

The anode was a lead foil previously preconditioned by overnight dipping in 1 mol dm^{-3} sulphuric acid to favour the formation of a passive layer. Lead contamination was not encountered during the experiments.

At least 60 cm^3 of solution was needed per experiment to keep the cathode properly immersed. A maximum of 450 cm^3 was treated with such a setup.

The electrolyte was not separated and the solution was exposed to air. The interelectrode gap was 0.5 ± 0.1 cm.

The remainder of the instrument arrangement was similar to the system used for the measurement of the diffusion coefficient (Section 2.3). Both types of control were investigated. The potential was held at -1.8 V vs SCE with a Luggin capillary to ensure a diffusion controlled zinc electrodeposition, whereas the current density based on the geometric surface area varied from 148 to 345 A m^{-2}, leading to potentials lower than -1.25 to -1.6 V vs SCE. The potentials investigated (-1.25 to -1.8 V vs SCE) which translate to -1.65 to -2.2 V vs Hg/Hg_2SO_4 (saturated with K_2SO_4) cover the range previously studied (Table 1).

The zinc concentration decrease was measured by periodically removing small samples (0.1 to 1 cm^3) from the reactor and analyzing them by atomic absorption (Section 2.1). This was not sufficient to significantly alter the volume of solution initially present in the reactor. It should be noted that the zinc deposited was compact, adherent and smooth. This is consistent with charge transfer controlled deposition. During diffusion controlled deposition, a powder was expected to form. However, the amount of zinc reduced during that period was not sufficient to initiate the appearance of powdery deposits [20]. In contrast to a typical roughness of 0.02 cm obtained with a RCER [2], zinc deposition during the diffusion controlled period was at most 0.69 g, representing a thickness of 0.0048 cm.

3. Results and discussion

3.1. *Reactions*

The following discussion deals with acid solutions (Table 1) but is also relevant to alkaline solutions. For example, zinc is plated from alkaline or cyanide baths [21] and a need may arise to clean the effluent before discharging. It is assumed that the reactor is separated to avoid explosive conditions between hydrogen and oxygen. Undivided reactors may be tolerated in laboratories since only very small amounts of gases are produced.

At the cathode, the reactions consist of zinc deposition,

$$Zn^{2+} + 2e^- \longrightarrow Zn \qquad (2)$$

hydrogen evolution,

$$2H^+ + 2e^- \longrightarrow H_2 \qquad (3)$$

oxygen reduction,

$$O_2 + 4H^+ + 4e^- \longrightarrow 2H_2O \qquad (4)$$

and impurity related reactions. These impurities may be metallic, thus codepositing with zinc, or organic,

$$M^{n+} + ne^- \longrightarrow M \qquad (5)$$

The organic substances may be subject to a reduction,

$$\text{Organic} + ne^- \longrightarrow \text{Products} \qquad (6)$$

or block the surface by preferential adsorption,

$$\text{Organic(bulk)} \longrightarrow \text{Organic(adsorbed)} \qquad (7)$$

After the detachment of the zinc particles from the cathode, corrosion can take place by either dissolved oxygen,

$$2Zn + O_2 + 4H^+ \longrightarrow 2Zn^{2+} + 2H_2O \qquad (8)$$

or hydrogen ions,

$$Zn + 2H^+ \longrightarrow Zn^{2+} + H_2 \qquad (9)$$

Several of the side reactions (Equations 3–9) may lead to drastic losses in zinc recovery and are easily suppressed by proper process control or selection. Aluminium is the material of choice for zinc electrowinning in sulfuric acid solutions [22]. However, since its hydrogen overpotential is lower than for zinc in the current density range of interest [23], it is necessary to plate zinc on aluminium if deposition is to be carried out from dilute solutions, otherwise practically only hydrogen evolves (Equation 3). Even with this precaution, the presence of Reaction 3 raises some doubt about a previously reported zinc deposition current efficiency value of 100% (Table 1).

Dissolved oxygen leading to a side reduction reaction and zinc corrosion is conveniently eliminated in the RCER by the evolving hydrogen bubbles, which act as a very effective means of desorption [18]. Therefore, even if the inlet electrolyte carries some dissolved oxygen, Reactions 4 and 8 may be disregarded if enough hydrogen is produced in the RCER [18]. However, at the drying stage, the importance of Reaction 8 needs to be emphasized and may explain the low purity of the zinc powder previously obtained (Table 1). As the liquid film surrounding the zinc particles gets thinner during the separation stage, the dissolved oxygen mass transfer is enhanced and may lead to a partly oxidized product unless special precautions are exercised. An alkaline alternative to the zinc electrowinning process offers some guidance. In such a case, a powder instead of a zinc plate is obtained which needs to be washed and dried [10–12, 24–29]. Since zinc powder is pyrophoric, making explosions possible, drying needs to be carried out under controlled conditions such as in an inert atmosphere or a vacuum.

Zinc electrowinning from sulfuric acid solutions is very sensitive to impurities (Equations 5–7) [30] and some of them, such as germanium and antimony, show a harmful effect at concentrations as low as a fraction of a mg dm^{-3}, leading to current efficiencies close to 0%. Therefore, it is more important that the electrolyte be relatively pure for dilute solutions, since current efficiency decreases rapidly with zinc concentration [22]. This conclusion may have consequences on process selection (Fig. 1). A selective solvent extraction step may be preferable (path *abf* or *abcd*)

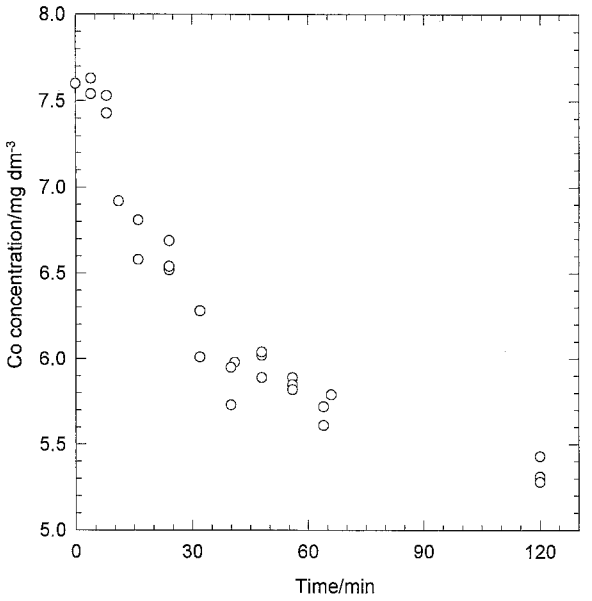

Fig. 3. Cobalt concentration decay data from three different experiments. Key: (○) 300, (□) 500 and (△) 700 mA. Solution a, 308 K, 5.23 g Zn added in one step (16 times the stoichiometric quantity required to remove all impurities).

to copper removal by cementation or using a RCER (path *ae*), since fewer impurities are expected to remain in the electrolyte. For example, cobalt present in the electrolyte (Table 2) cements with difficulty [31] as shown in Fig. 3. The same final result of 5 mg dm^{-3} is obtained independently of the experimental conditions used here. By comparison, copper, which is more concentrated (Table 2), was easily removed to a level of 0.1 mg dm^{-3} under the same experimental conditions [15]. At a level of 5 mg dm^{-3}, cobalt may still be deleterious since it is known to exhibit an incubation period [31] beyond which its effect on current efficiency is much more pronounced. The incubation period has also been linked to the roughening of the zinc deposit [32]. These factors are critical for the continuous operation and deposition of powders in a RCER and show the need for a relatively pure electrolyte.

Finally, acid corrosion of the zinc powder may also arise (Equation 9). This reaction, however, is very slow if the zinc is sufficiently pure [23], due to a large hydrogen overpotential. If the zinc is contaminated with impurities having low hydrogen overpotentials, such as cobalt or iron (Table 2) [23, 30], the corrosion reaction is much more rapid [23] and again shows the need for proper electrolyte purification. Anomalous codeposition, a phenomenon of concern in the alloy plating industry [21], is also of interest in zinc removal. Zinc is known to show anomalous codeposition with metals such as iron or cobalt (Table 2) [33], whereby the zinc preferentially deposits with respect to the more noble metals. This increases zinc purity and leads to reduced corrosion of the zinc particles. If other impurities are present, such as arsenic (Table 2) [33], this trend may be slightly reversed. It is noteworthy that in connection with alkaline zinc based batteries, zinc powder corrosion occurring during storage was previously studied [34–36]. These studies are useful with respect to the methods considered and the parallel which can be established with acid corrosion.

3.2. *Rotating cylinder electrode reactor behaviour*

The behaviour of a batch reactor at an imposed current leading to charge transfer controlled zinc deposition is [37],

$$c_{Zn}(t) = c_{Zn}(0) - \frac{\phi It}{nFV} \tag{10}$$

Therefore, a plot of $c_{Zn}(t)$ against t leads to a linear relationship whose slope allows determination of the zinc deposition current efficiency.

After the zinc concentration has somewhat decreased, the imposed current leads to diffusion controlled zinc deposition and the reactor behaviour is given by [37]:

$$c_{Zn}(t) = c_{Zn}(0)\exp(-kA_c t/V) \tag{11}$$

Thus, a plot of log $c_{Zn}(t)$ against t leads to a linear relationship which, in turn, allows determination of k from its slope. Since zinc is deposited at its limiting current,

$$I_l = nFkA_c c_{Zn}(t) \tag{12}$$

the zinc deposition current efficiency is obtained,

$$\phi = \frac{nFkA_c c_{Zn}(t)}{I} \tag{13}$$

Also, if Equation 11 is introduced in Equation 13, the zinc current efficiency shows a linear behaviour if log ϕ is plotted against t. In the case of a batch reactor operated potentiostatically in the diffusion controlled zinc deposition region, only Equation 11 remains valid and a charge transfer controlled region (Equation 10) is not observed.

Since turbulent mass transfer to a smooth cylinder is given by the following dimensionless correlation [4]:

$$Sh = 0.079\, Re^{0.7} Sc^{0.356} \tag{14}$$

the zinc diffusion coefficient is determined using the k value and is given in Table 3. The kinematic viscosity measured for the synthetic solution at pH 4 was used to compute the zinc diffusion coefficient for solution *e* (Table 3). For solutions *f* and *d*, the kinematic viscosity measured for the 1 mol dm^{-3} synthetic sulfuric acid solution was used (Table 3).

In the presence of powdered metal deposits, Equation 14 needs to be modified by replacing the *Re* exponent by 0.92 [4]. In this case, the mass transfer coefficient is increased substantially compared to when the surface is smooth, and leads to a faster decay of the concentration (k is increased in Equation 11). This manifests itself on a log $c_{Zn}(t)$ against t plot by the eventual appearance of a second linear relationship with a higher slope [2]. However, this behaviour was not observed here since zinc was not deposited in powdered form, as explained in Section 2.5.

Equation 14 was previously shown to be generally applicable in the presence of mass transfer contributions such as axial flow (single pass reactor) or parallel

bubble evolution (hydrogen) [38]. At sufficiently large hydrogen current densities however, bubbles have an effect [39] and Equation 14 is no longer valid under these conditions. The critical hydrogen current density beyond which bubble mass transfer must be taken into account was previously expressed as [18]:

$$j = 2.67 \times 10^{-4}\omega^{1.33} \quad (15)$$

and leads to a value of 2430 A m^{-2} at 168 rad s^{-1} (Section 2.5). This is approximately one order of magnitude larger than the highest applied current density used here (345 A m^{-2}, Section 2.5).

3.3. *Synthetic solutions*

Zinc concentration decay curves are illustrated in Fig. 4 for several imposed currents. Two different regions are observed corresponding, respectively, to charge transfer and diffusion control as discussed in Section 3.2. The zinc deposition current efficiency and mass transfer coefficient found using Equations 10 and 11, respectively, are given in Table 3.

Zinc deposition current efficiency is plotted in Fig. 5 for several imposed currents. Again, two different regions are distinguished as in Fig. 4, and follow the expected behaviour determined from Equations 10, 11 and 13. It is noteworthy that even if a pH of approximately zero were used, a value lower than in previous attempts (Table 1), zinc is still removed with a good current efficiency at low concentrations in the charge transfer control region. This is partly attributable to the good agitation provided by the RCER. In the diffusion control region, beginning at residual concentration levels varying from 2000 to 3000 mg dm^{-3} (Fig. 4), the zinc deposition current efficiency decreases rapidly (Equation 13) and a substantial amount of energy is lost on account of hydrogen evolution which maintains the imposed current.

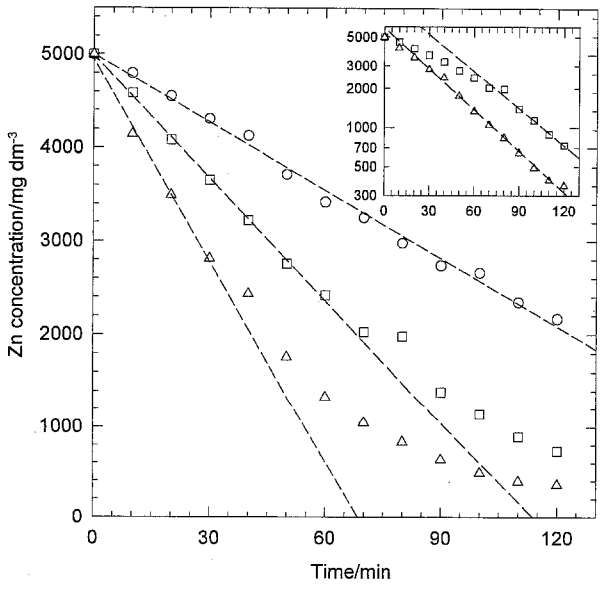

Fig. 4. Zinc concentration decay curves for synthetic solutions at different applied currents. The inset figure represents some of the data on a semi-logarithmic scale. 5 g dm^{-3} Zn as $ZnSO_4.7H_2O$+ 1 mol dm^{-3} H_2SO_4 at 295 K, 100 cm^3 and 1600 r.p.m. Key: (○) 300, (□) 500 and (△) 700 mA.

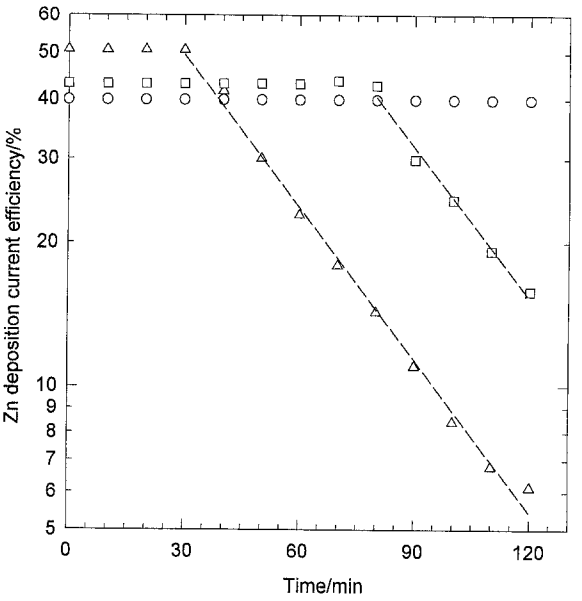

Fig. 5. Zinc deposition current efficiency for synthetic solutions as a function of time at different applied currents. Concentrations, conditions and key as for Fig. 4.

Therefore, a potentiostatic operation with fixed hydrogen current is industrially preferable. This type of control was found to lead to similar concentration decay curves. Furthermore, the zinc deposition current efficiency is found to increase with the applied current in the charge transfer control region (Fig. 5). This is consistent with the Tafel slopes found for both major reactions taking place in the RCER. The Tafel slope at 295 K for zinc deposition is 73 mV decade^{-1} whereas it is 117 mV decade^{-1} for hydrogen evolution [40]. Therefore, as the current increases, the zinc deposition current rises more rapidly than the hydrogen evolution current, resulting in a higher zinc deposition current efficiency.

The value of the zinc diffusion coefficient derived from the mass transfer coefficient (Table 3) does not agree with the value found using a rotating disc electrode (Section 2.3). Also, both of these diffusion coefficients are much lower than the reported value of 4.72×10^{-6} cm^2 s^{-1} at 295 K (0.01 to 0.15 mol dm^{-3} $ZnSO_4$ + 0.2 mol dm^{-3} Na_2SO_4, pH 4.77 to 5.68 at 298 K) [41]. This is due to ion pair formation [41–44],

$$Zn^{2+} + SO_4^{2-} \longrightarrow ZnSO_4^0 \quad (16)$$

which has a formation constant of 240 mol^{-1} dm^3 at 298 K and infinite dilution [43]. In Figs 4 and 5, due to the use of high concentration of sulfate ions, the equilibrium of Equation 16 is displaced to the right and the concentration of zinc ions is low. This leads to a low zinc diffusion coefficient value when larger analytical zinc concentrations are used to plot the data. This simple analysis is sufficient here; a complete discussion of the problem of diffusion controlled metal deposition reactions in the turbulent regime preceded by a homogeneous chemical reaction is beyond the scope of the present paper. In addition, an independent measurement of the diffusion coefficient is required to correlate the data according to Equation 14. However, since the usual methods such as the

rotating disc electrode also require knowledge of the concentration which was undetermined here, such a correlation could not be attempted without an extensive effort which, again, was judged beyond the scope of the present paper.

Correlation of the zinc deposition current efficiency was previously attempted in the electrowinning industry and led to the conclusion that it is mainly dependent on the zinc sulphate to sulfuric acid concentration ratio for pure solutions [45, 46]. This correlation, Wark's rule, takes the following form [45, 46]:

$$\frac{\phi}{1-\phi} = K\frac{c_{Zn}}{c_H} \qquad (17)$$

The data of Figures 4 and 5 were plotted according to Equation 17 in Fig. 6 and were not corrected for acid formation in the batch reactor since they represented at the most a 7.1% change. Equation 17 with $K = 13.31$ (best fit) is also plotted in Fig. 6 and shows that Wark's rule is not followed for dilute zinc solutions. A careful analysis of a theoretical Wark's rule derivation [47] reveals that it fails for two major reasons. Diffusion is not taken into account and it was assumed that the salt and acid dissociation coefficients are proportional to the respective concentrations. These assumptions are not valid here since zinc deposition is diffusion controlled over a fairly large concentration range (Equation 11, Fig. 4) and the dissociation coefficient is not proportional to the concentration, as evidenced by some data for dilute zinc solutions [41].

3.4. *Process solutions*

Figures 7 and 8 show that for the solutions obtained after solvent extraction (*f* and *d*, Fig. 1), zinc concentration decay curves and zinc deposition current efficiency follow the same behaviour as synthetic solutions (Figs 4 and 5). However, a lower current efficiency is obtained in the absence of an activated carbon cleaning step in the charge transfer control region (Table 3). The extractant used has a purity of 84% and, since its solubility in water is very low, the more soluble organic impurities constituting the remaining 16% partly find their way into solution *f* [15]. Since copper is effectively removed by chromatography ($<0.2\,mg\,dm^{-3}$) [15] and zinc extraction is selective, in particular with respect to cobalt [15], the concentration of the metallic impurities present (Table 2) is probably decreased below levels likely to cause harmful effects. It is also observed that the current efficiency remains constant for nearly the first three hours of electrolysis (Fig. 8). It can be deduced

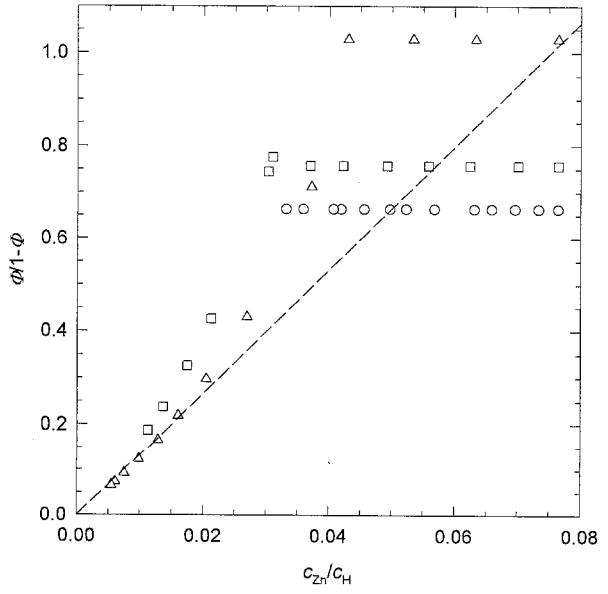

Fig. 6. Experimental verification of the validity of Equation 17 (Wark's rule). Concentrations, conditions and key as for Fig. 4.

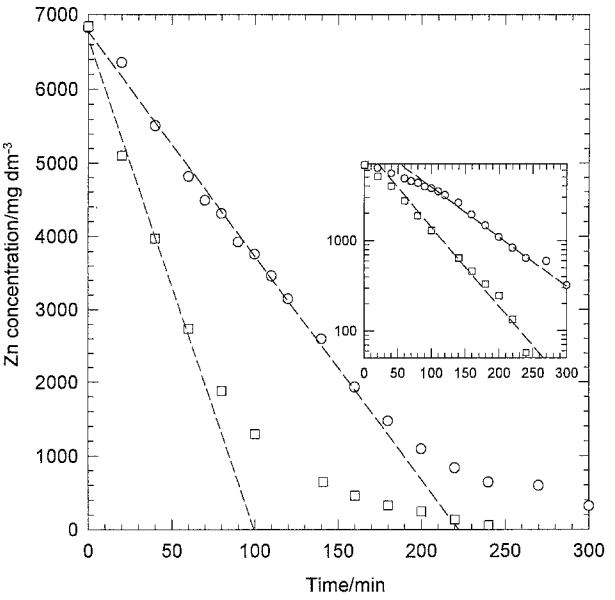

Fig. 7. Zinc concentration decay curves for the solution obtained after the solvent extraction step in both the absence (solution *f* (○), 70 cm^3) and presence (solution *d* (□), 63 cm^3) of an activated carbon cleaning step. The inset figure represents the same data on a semi-logarithmic scale. 6.8 g dm^{-3} Zn as $ZnSO_4.7H_2O$ + 1 mol dm^{-3} H_2SO_4 at 295 K, 1600 r.p.m. and 500 mA.

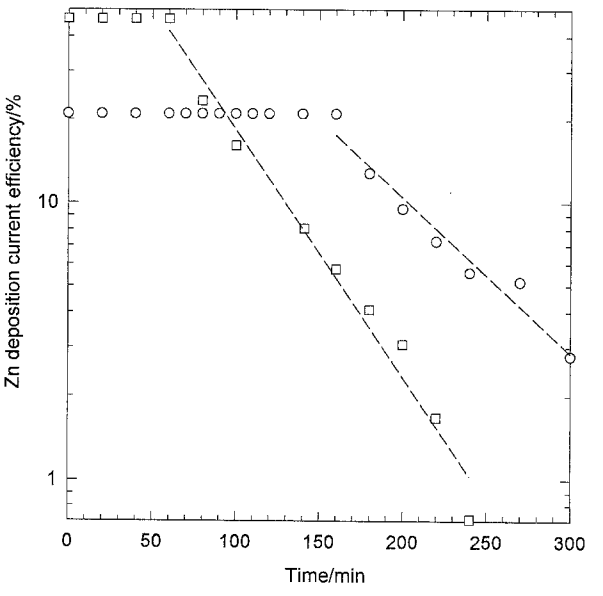

Fig. 8. Zinc deposition current efficiency for the solution obtained after the solvent extraction step as a function of time in both the absence (solution *f*) and presence (solution *d*) of an activated carbon cleaning step. Concentrations, conditions and key as for Fig. 7.

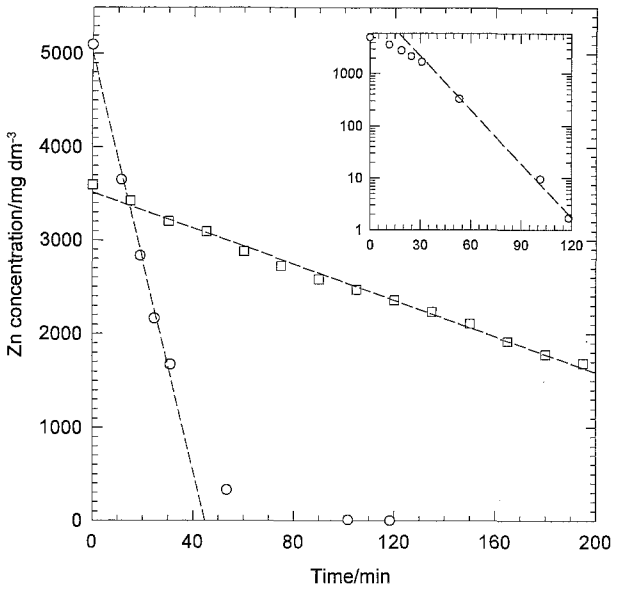

Fig. 9. Zinc concentration decay curves for solution *e* obtained after the copper removal step carried out either by cementation or by using a RCER. The inset figure represents some of the data on a semi-logarithmic scale. Key: (O) Cu removed by cementation (5.1 g dm^{-3} Zn, 70 cm^3); (□)Cu removed with a RCER (3.8 g dm^{-3} Zn, 450 cm^3). Conditions: 295 K, 1600 r.p.m., 500 mA.

that the organic impurities are most likely not subject to any reduction (Equation 6), otherwise the current efficiency would have changed. Adsorption of organic substances (Equation 7) is favoured at potentials which are slightly negative to the point of zero charge [48]. For zinc, this potential is −0.63 V vs SHE [49], near the deposition potential values used here (−1.06 to −1.31 V vs SHE). The adsorbed organics can disrupt zinc deposition kinetics [48, 50], leading to smaller current efficiencies. If a cleaning step is used to remove the dissolved organics, the zinc deposition current efficiency in the charge transfer control region is similar to the value obtained for synthetic solutions (Fig. 8 and Table 3).

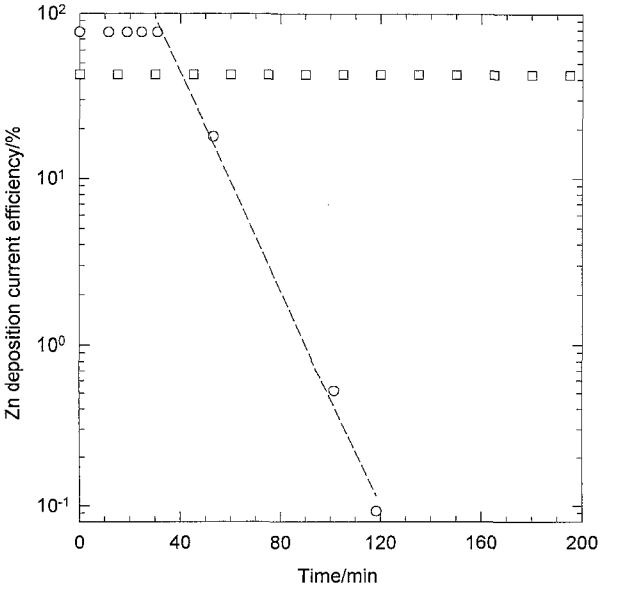

Fig. 10. Zinc deposition current efficiency for solution *e* obtained after the copper removal step carried out either by cementation or by using a RCER as a function of time. Key and conditions as for Fig. 9.

Again, low zinc diffusion coefficients are observed for solutions *f* and *d* (Table 3) due to a high sulfuric acid concentration displacing the ion pair formation equilibrium (Equation 16) to the right (Section 3.3).

Figures 9 and 10 illustrate that for solutions originating from the copper removal step (*e*, Fig. 1), both zinc concentration and current efficiency exhibit the same behaviour as for synthetic solutions (Figs 4 and 5). However, use of an RCER for copper removal leads to lower current efficiencies in the charge transfer control region (Fig. 10). In this case, the RCER can be used to obtain a marketable product not contaminated by more electroactive impurities (Table 2) [16]. These metallic impurities still present in the solution decrease zinc deposition current efficiency and purity (Section 3.1). Indeed, at the beginning of the experiment a slight amount of black powder, indicative of diffusion controlled deposition [20], is formed, revealing that the RCER treatment is inadequate for the removal of all impurities which are less electroactive than zinc (Table 2) [16]. After powder removal from the working electrode, zinc deposition occurs without further problems, as shown in Fig. 9.

If cementation is used, most impurities including copper, are removed to sufficiently low levels, resulting in a purer solution and a larger zinc deposition current efficiency in the charge transfer control region (Fig. 10 and Table 3). The current efficiency in the charge transfer control region is also greater than for synthetic solutions since the pH is higher [22]. Most importantly, very low zinc concentrations are reached (~2 mg dm^{-3}), lower than in previous attempts (Table 1) if sufficiently pure solutions are used. This point remains to be proven for longer operating times involving powder deposition, since deleterious impurity effects may manifest themselves under these conditions (Section 3.1). The zinc diffusion coefficient appears reasonable (Table 3), due to less sulfate in the electrolyte, which does not favour formation of a zinc ion pair (Equation 16). Finally, even when a better current efficiency is achieved after cementation, the solution conductivity is lower than for solutions generated by solvent extraction (Table 3) for which better conductivities are expected. Therefore, from a specific energy consumption point of view, there may be no advantage in using either of these processes.

4. Conclusion

It has been demonstrated that zinc removal with a RCER follows expected behaviour and that both low pH and zinc concentration can be used if the solutions are substantially pure. However, a number of important issues still need to be addressed to further assess the technology. These include zinc ion pair formation and insufficient or absent data on several aspects such as zinc powder corrosion and purity, and RCER continuous operation under powder formation conditions.

Acknowledgements

We are grateful to Environeau Inc. for the financial aspects related to the production of this manuscript. Thanks are also extended to Louise Noreau for cementation experiments and Andrea Corwin for grammatical corrections.

References

[1] D. R. Gabe, *J. Appl. Electrochem.* **4** (1974) 91.
[2] D. R. Gabe and F. C. Walsh, *ibid.* **13** (1983) 3.
[3] N. A. Gardner and F. C. Walsh, *in* 'Electrochemical Cell Design' (edited by R. E. White), Plenum Press, New York (1984), p. 225.
[4] F. C. Walsh, *in* 'Electrochemistry for a Cleaner Environment' (edited by J. D. Genders and N. L. Weinberg), Electrosynthesis Company Incorporated, East Amherst, New York (1992) p. 101.
[5] L. E. Vaaler, *J. Electrochem. Soc.* **125** (1978) 204.
[6] F. S. Holland, *Chem. Ind., (London)* (1978) 453.
[7] *Idem, British Patent 1 444 367* (1976).
[8] *idem, US Patent 4 028 199* (1977).
[9] *Idem, British Patent 1 505 736* (1978).
[10] G. W. Johnson, *British Patent 506 590* (1939).
[11] H. J. Morgan and J. D. Gray, *Eng. Mining J.* **151** (1950) 72.
[12] J. Prunet and A. Guillen, *French Patent 1 264 597* (1961).
[13] M. Bergeron, R. Boisvert, S. Chevé, J. Cyr, D. Germain, M. Piotte, N. Massé, K. Oravec and N. Tassé, 'Restauration et Revalorisation de Parcs de Résidus Miniers', PMC-II Project, Report 1, INRS–Géoressources, Ste-Foy, Québec (1992).
[14] PMC-II team, 'Restauration et Revalorisation de Parcs de Résidus Miniers', PMC-II Project, Report 2, INRS–Géoressources, Ste-Foy, Québec (1993).
[15] INRS-Géoressources, 'Restauration et Revalorisation de Parcs de Résidus Miniers', PMC-II Project, Final Report, INRS-Géoressources, Ste-Foy, Québec (1993).
[16] N. Massé, J. St-Pierre and M. Bergeron, *J. Appl. Electrochem.* **25** (1995) 340.
[17] J. St-Pierre, N. Massé and M. Bergeron, *Electrochim. Acta* **39** (1994) 2705.
[18] J. St-Pierre, N. Massé and M. Bergeron, *ibid.* **40** (1995) 1013.
[19] Yu. V. Pleskov and V. Yu. Filinovskii, 'The Rotating Disk Electrode', Consultants Bureau, New York (1976).
[20] F. C. Walsh and M. E. Herron, *J. Phys. D: Appl. Phys.* **24** (1991) 217.
[21] F. A. Lowenheim, 'Electroplating', McGraw-Hill, New York (1978).
[22] A. C. Scott, R. M. Pitblado, G. W. Barton and A. R. Ault, *J. Appl. Electrochem.* **18** (1988) 120.
[23] M. Pourbaix, 'Atlas of Electrochemical Equilibria in Aqueous Solutions', National Association of Corrosion Engineers, Houston, Texas (1974).
[24] W. Eckardt, US Bureau of Mines IC 7466 (1948).
[25] C. T. Baroch, R. V. Hilliard and R. S. Lang, *J. Electrochem. Soc.* **100** (1953) 165 and 590.
[26] C. C. Merrill and R. S. Lang, US Bureau of Mines RI 6576 (1965).
[27] R. L. Meek, *in* 'Electrometallurgy' (edited by T. A. Henrie and D. H. Baker), The Metallurgical Society of AIME, New York (1969) p. 306.
[28] W. W. Anderson, H. P. Rajcevic and W. R. Opie, 'Pilot Plant Operation of the Caustic Leach-Electrowin Zinc Process', 110th Annual AIME Meeting, Chicago, Illinois, Feb. 1981, Paper A81-52, The Metallurgical Society of AIME, Warrendale, PA.
[29] J. N. Frenay and J. Hissel, *ATB Métallurgie* **24** (1984) 233.
[30] D. J. Mackinnon, J. M. Brannen and P. L. Fenn, *J. Appl. Electrochem.* **17** (1987) 1129.
[31] J. D. Miller, *in* 'Metallurgical Treatises' (edited by J. K. Tien and J. F. Elliot), The Metallurgical Society of AIME, Warrendale, PA (1981), p. 95.
[32] N. Massé and D. L. Piron, *J. Appl. Electrochem.* **20** (1990) 630.
[33] H.-M. Wang and T. J. O'Keefe, *ibid.* **24** (1994) 900.
[34] R. N. Snyder and J. J. Lander, *Electrochem. Technol.* **3** (1965) 161.
[35] P. Rüetschi, *J. Electrochem. Soc.* **114** (1967) 301.
[36] R. V. Moshtev and R. Stoicheva, *J. Appl. Electrochem.* **6** (1976) 163.
[37] F. C. Walsh, 'A First Course in Electrochemical Engineering', The Electrochemical Consultancy, Romsey, Hampshire, UK (1993).
[38] K. Scott, 'Electrochemical Reaction Engineering', Academic Press, London (1991).
[39] B. Roald and W. Beck, *J. Electrochem. Soc.* **98** (1951) 277.
[40] G. W. Barton and A. C. Scott, *J. Appl. Electrochem.* **22** (1992) 104.
[41] I. Zouari and F. Lapicque, *Electrochim. Acta* **37** (1992) 439.
[42] F. Ajersch, D. Mathieu and D. L. Piron, *Can. Met. Quart.* **24** (1985) 53.
[43] H. Majima, E. Peters, Y. Awakura and S. K. Park, *Metall. Trans. B.* **18B** (1987) 41.
[44] S. Wasylkiewicz, *Fluid Phase Equilibria* **57** (1990) 277.
[45] I. W. Wark, *J. Appl. Electrochem.* **9** (1979) 721.
[46] T. Biegler and E. J. Frazer, *ibid.* **16** (1986) 654.
[47] G. C. Bratt, *in* 'Tasmania Conference 1977', Australasian Institute of Mining and Metallurgy, Melbourne (1977), p. 277.
[48] J. O'M. Bockris and A. K. N. Reddy, 'Modern Electrochemistry', Vol. 2, Plenum Press, New York (1970).
[49] K. J. Vetter, 'Electrochemical Kinetics', Academic Press, New York (1967).
[50] L. Antropov, 'Électrochimie Théorique', Mir, Moscow (1979).